Investigation of permanent magnets in low-cost position tracking

Ryan Anderson, Andras Lasso, Keyvan Hashtrudi-Zaad, Gabor Fichtinger

Queen's University, Kingston Ontario

ABSTRACT

PURPOSE**:** Low cost portable ultrasound systems could see improved utility if similarly low cost portable trackers were developed. Permanent magnet based tracking systems potentially offer adequate tracking accuracy in a small workspace suitable for ultrasound image reconstruction. In this study the use of simple permanent magnet tracking techniques is investigated to determine feasibility for use in an ultrasound tracking system. METHODS**:** Permanent magnet tracking requires finding a position input into a field model which minimizes the error between the measured field, and the field expected from the model. A simulator was developed in MATLAB to determine the effect of sources of error in permanent magnet tracking systems. Insights from the simulations were used to develop a calibration and tracking experiment to determine the accuracy of a simple and low cost permanent magnet tracking system. RESULTS**:** Simulation and experimental results show permanent magnet based tracking to be highly sensitive to errors in sensor measurements, calibration and experimental setup. The reduction in field strength of permanent magnets lowers with the cube of distance, which leads to very poor signal-to-noise ratios at distances above 20 cm. Small errors in experimental setup also led to high tracking error. CONCLUSION**:** Permanent magnet tracking was found to be less accurate than is clinically useful, and highly sensitive to errors in sensors and experimental setup. Sensor and calibration limitations make simple permanent magnet tracking systems a poor choice given the present state of sensor technology.

Keywords: magnetometer, tracking, computer assisted surgery

PURPOSE

Tracked 3D ultrasound has shown excellent potential to improve outcomes in many interventions. However, tracking continues to be expensive and often cumbersome. Permanent magnet tracking for medical use has been demonstrated as early as 1997[1] using large super-cooled sensors. More recently MEMS-based sensors have drastically reduced the cost and complexity of magnetic field measuring tools. Published methods tend to use very large numbers of sensors in fixed planar arrays or sets of planar arrays[2]. In this study, we investigated the feasibility of simple and low cost permanent magnet tracking solutions using only one sensor and magnet. The goal was to achieve less than 5 mm position error in a 30x30x30 cm workspace which is adequate for 3D reconstruction and simple guided interventions.

METHODS

The objective in permanent magnet tracking is to find a position coordinate of the magnet which minimizes the error between the measured magnetic field and the field expected from a model. The model used in this work is the dipole model shown in Equation 1. The dipole model is simple to compute and approximates the field of the cylindrical magnet used in the far field.

$$\vec{B}(m,\vec{r},\vec{H}) = \frac{\mu_0 m}{4\pi}\left(\frac{3r(\vec{H}\cdot\vec{r})}{|\vec{r}|^5} - \frac{\vec{H}}{|\vec{r}|^3}\right) \quad (1)$$

The dipole model is a function of m, a scalar value proportional to the strength of the magnet, $\vec{r}$ the vector from the magnet to the sample point, and $\vec{H}$ the orientation of the magnet. The vector $\vec{H}$ lies on the axis of rotational symmetry of the cylindrical magnet, pointing towards the direction with positive magnetic field. The value $\vec{B}$ is measured in Gauss and is the magnetic field vector at the sample point. Figure 1 shows the relationships of the vectors used in the dipole equation for an example where two sensors are used.

In this study tracking is done in 3 position dimensions only, with the magnet orientation $\vec{H}$ being known, as well as the strength m. The tracking problem then is to find a value of $\vec{P}_{mag}$ which minimizes the error function in Equation 3. The results shown in this study used one sensor but the multisensory equations are shown for generality, with N sensors. As the sensor locations are known in the solution frame, a single estimate of $\vec{P}_{mag}$ is required to determine each vector $\vec{r}_n$ using Equation 2. The optimization was done using the Levenberg-Marquardt (LM) algorithm, which reduces the cost function shown in Equation 3.

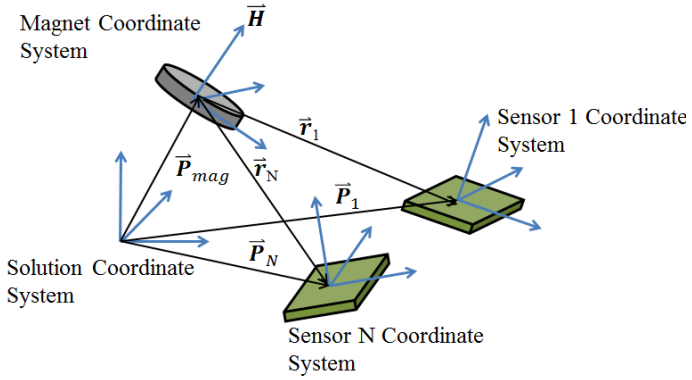

Figure 1. Coordinate system diagram of sensors and magnet.

$$\vec{P}_{mag} = \vec{P}_n - \vec{r}_n \quad (2)$$

$$Error(\vec{r}) = \sum_{n=1}^{N} \left(\vec{B}_n - \vec{B}_{mod}(\vec{r}_n)\right)^2 \quad (3)$$

The LM algorithm requires two inputs, a choice of damping parameter and an initial guess of the solution. The choice of damping parameters causes the LM algorithm to approach the Gauss-Newton algorithm or Gradient Descent algorithm. In the MATLAB implementation used this value is modified automatically to provide faster convergence[4]. For the experiments and simulations shown here the magnet followed a continuous trajectory. For the first point on its path the optimizer was provided a reasonable position guess, and for all subsequent points the previously solved position was used as the initial guess.

The sensor used was a PhidgetSpatial Precision 3/3/3, a combined 3-axis magnetometer, accelerometer and gyroscope which retails for $140.00. The permanent magnet used was a 1/8th inch thick by ¾ inch diameter rare-earth grade N52 permanent cylindrical magnet. In this study 3D tracking using this sensor was performed experimentally, and a simulation was developed in MATLAB. The purpose was to deterrmine the feasibility of using limited numbers of sensors in simple configurations for tracked ultrasound applications.

The tracking experiment was performed with the magnet and sensor rigidly attached to mounts which fit into a perforated board. The solution coordinate frame was defined by the peg board as

shown in Figure 2, and is referred to as the peg coordinate system. The magnet and sensors positions and orientations are known in the peg coordinates from their positions on the peforated board. To ensure high tracking accuracy, the sensor and the experimental setup were calibrated prior to performing position tracking experiments. The error model of the sensor is shown in Equation 4.

$$\vec{\boldsymbol{B}}_{sensor} = \boldsymbol{s}\left(\vec{\boldsymbol{B}}_{true}\right) + b + e \tag{4}$$

The sensor error model accounts for linear scaling $\boldsymbol{s}$ in each sensor axis**,** bias b and noise e which modify the measured value $\vec{\boldsymbol{B}}_{sensor}$ of the actual field $\vec{\boldsymbol{B}}_{true}$. Not shown in the equation is the sensor resolution which is the minimum units of magnetic field the sensor can measure. For the sensor used here the resolution is 3 milligauss (mg), for reference the Earth's magnetic field is approximately 600 mg. These error parameters are solved using a calibration software tool provided by the sensor manufacturer.

a) Detail of magnet and sensor mounts

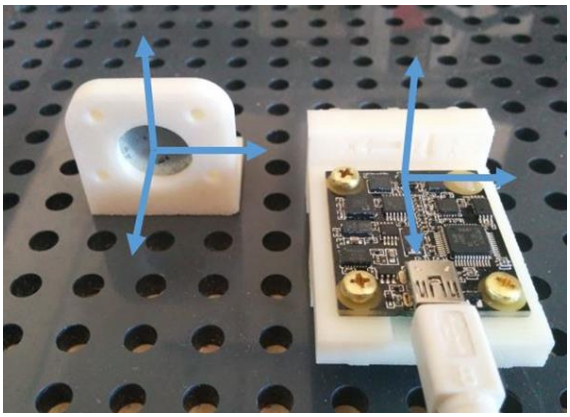

b) Overhead view of data collection space

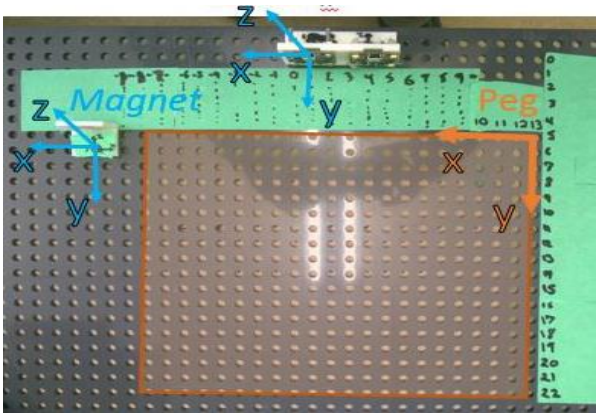

Figure 2. Data collection board **b)** with detail of magnet and sensor mounts **a).**

In the tracking experiments, the ground truth values of the magnet and sensor positions are known from the location of their mounts on the perforated board. There are small errors in their assumed position and orienation realtive to their mounts which must be considered for an accurate ground truth to be known. As the mounts were made to fit into the holes of the board at each point, it is assumed that these errors are consistent across every sample point. These errors were be solved for my minimizing Equation 5.

$$\boldsymbol{Error}\left(m, \vec{\boldsymbol{H}}, \vec{\boldsymbol{e}}_{sensor}, \vec{\boldsymbol{e}}_{mag}, R^{peg}_{sensor}, \boldsymbol{s}\right) = R^{peg}_{sensor}\boldsymbol{s}\vec{\boldsymbol{B}}^{sensor}_{meas} - \vec{\boldsymbol{B}}^{peg}_{model}\left(m, \vec{\boldsymbol{H}}, \vec{\boldsymbol{r}}\right) \tag{5}$$

$$\vec{\boldsymbol{r}} = \left(\vec{\boldsymbol{p}}^{peg}_{sensor} + \vec{\boldsymbol{e}}_{sensor}\right) - \left(\vec{\boldsymbol{p}}^{peg}_{mag} + \vec{\boldsymbol{e}}_{mag}\right) \tag{6}$$

The error in the expected position of the magnet and sensor are given by $\vec{\boldsymbol{e}}_{sensor}$ and $\vec{\boldsymbol{e}}_{mag}$. The rotation error of the magnet is accounted for by correcting its direction vector $\vec{\boldsymbol{H}}$ as measured in the peg coordinate frame, while the sensor is rotated by the rotation matrix R^{peg}_{sensor} which fits the sensor coordinate frame to the peg coordinate frame. The scalar strength of the magnet and scaling errors of the sensor are given by m and $\boldsymbol{s}$ respectively. These errors were solved by comparing collected data at known points on the pegboard to expected data from the field model.

The LM algorithm was used to find a single set of error parameters that minimized the error of all collected calibration data simultaneously.

Sensor Calibration

The sensors were first calibrated using the manufacturer's calibration software tool. This tool uses the expected background field as a ground truth, and attempts to match the measured fields to this. First, the expected background field was found using published geological data from NASA for the area the experiment was performed (http://www.ngdc.noaa.gov/geomag-web/). The sensor is then rotated about in space to collect multiple points from each of the 3-axis sensors. The magnetic field vectors if plotted should show a sphere, as the vector will always be of the same magnitude regardless of sensor orientation. Due to errors in the sensor gain, bias and orientation, the actual shape plotted will be some form of ellipsoid. The software then determines the gain, bias and rotation to apply to fit this ellipsoid to a sphere defined by the magnitude provided by the user. The results of this calibration are gain and bias parameters for each sensor, and six factors which describe the non-orthogonality of the measured ellipse. The orientation of the sensors relative to the earth field is determined using the built in gyroscopes and accelerometers, and as a result there is some error in this. As well, to achieve an accurate calibration, the background field must be known accurately and must be homogenous in the space the probe is calibrated in. As neither of these condition can be met, this calibration had to be further refined using more robust methods.

The manufacturer's calibration method assumes the background field in the calibration area is known and is homogenous within the area the sensor is calibrated in. As magnetic field tracking solutions require a high degree of accuracy in the sensors, this calibration was further refined using experimental data. Before any data was collected, the manufacturer's calibration was performed in the area the sensor would be mounted for further data collection. The manufacturer's calibration pre-filters the raw data, therefore all further calibrations are applied to sensor data which has already been initially filtered.

In the calibration used, the sensors and magnet were kept in the same orientation relative to the pegboard. The sensors remained stationary, and the magnet was moved across the pegboard grid to collect multiple sample points. After placing the sensors on the data collection setup, the background field of the room was collected for 10 seconds and averaged. At each position, the sensor collected data for 4 seconds at 125 samples per second. The raw data was averaged to remove high frequency noise, and the previously collected background field was subtracted leaving a measurement of only the field of the permanent magnet. By leaving the sensors stationary, the background magnetic field does not change during the data collection allowing the initial measurement of the background field to be used to correct future measurements.

Calibration was done specifically to calibrate the setup for a tracking experiment where it is desired to know the position and orientation of the sensors and magnets relative to the measurement coordinate system. The ground truth position and orientation values of the sensor and magnet are determined form the positions in which they are mounted on the pegboard. Errors in these positions and orientations introduce systematic errors that reduce the ability to accurately measure the true tracking performance of the system. A calibration refinement was done to reduce the error in the assumed ground truth positions and oreintations of the magnet and sensor to improve the ability to correctly measure the tracking accuracy. The strength of the magnet estimated during this calibration as well to fit the measured data, along with scaling

errors in each sensor axis. Because there is no independent measurement available for the magnetic field values, all of these error sources are solved simultanesouly to find parameters that provide the best fit to the measured data.

$$\boldsymbol{E}\left(m, \vec{\boldsymbol{H}}, \vec{\boldsymbol{e}}_{sensor}, \vec{\boldsymbol{e}}_{mag}, R^{peg}_{sensor}, \boldsymbol{s}\right) = R^{peg}_{sensor}\boldsymbol{s}\vec{\boldsymbol{B}}^{sensor}_{meas} - \vec{\boldsymbol{B}}^{peg}_{model}\left(m, \vec{\boldsymbol{H}}, \vec{\boldsymbol{r}}\right) \tag{7}$$

$$\vec{\boldsymbol{r}} = \left(\vec{\boldsymbol{p}}^{peg}_{sensor} + \vec{\boldsymbol{e}}_{sensor}\right) - \left(\vec{\boldsymbol{p}}^{peg}_{mag} + \vec{\boldsymbol{e}}_{mag}\right) \tag{8}$$

The goal of this optimization is to find error parameters that best fit a measurement from the sensor $\vec{\boldsymbol{B}}^{sensor}_{meas}$ to an expected field at that point from the field model $\vec{\boldsymbol{B}}^{peg}_{model}$. The dipole model requires knowing the magnet orientation $\vec{\boldsymbol{H}}$ and the vector from the magnet to the sample point $\vec{\boldsymbol{r}}$, both measured here in the pegboard's coordinate system. The position of the sensor in pegboard coordinates is given by it's assumed position relative to the pegboard $\vec{\boldsymbol{p}}^{peg}_{sensor}$ plus some systematic error position error $\vec{\boldsymbol{e}}_{sensor}$. Similarly the magnet position plus position error is in pegboard coordinates defined by $\vec{\boldsymbol{p}}^{peg}_{mag} + \vec{\boldsymbol{e}}_{mag}$. To compare modelled field values to those measured, the measurements from the sensor must be scaled and rotated to the pegboard coordinate system. The rotation is given by R^{peg}_{sensor} and the scaling in each measurement axis by $\boldsymbol{s} = [s_x, s_y, s_z]$. Lastly the strength of the magnet is given by the scalar value m.

The Levenberg-Marquardt algorithm was used to solve for the error parameters, with a damping λ_0 of 0.01. The parameters were solved iteratively to begin with, with all of the intial guesses assuming zero error. As each parameter was solved, it's solution was used for the following optimizations. The parameters were solved in the following order: magnet strength, sensor scaling, magnet position error, magnet orientation, sensor position error, sensor orientation. After each parameter was solved in this method, the optimizer was run to solve all parameters simultaneously with the iteratively sovled values as the initial guess. This method was chosen as it was found that optimizer did not always return sensible values for position and orientation errors if the magnet strength and sensor scaling were not solved intially, and the optimizer would have difficulty converging without close initial guesses. The correction can be visualized by plotting the measured data against the expected data, as seen in Figure 3. If the model is a perfect fit, all of the data points will lie on the line given by $x = y$.

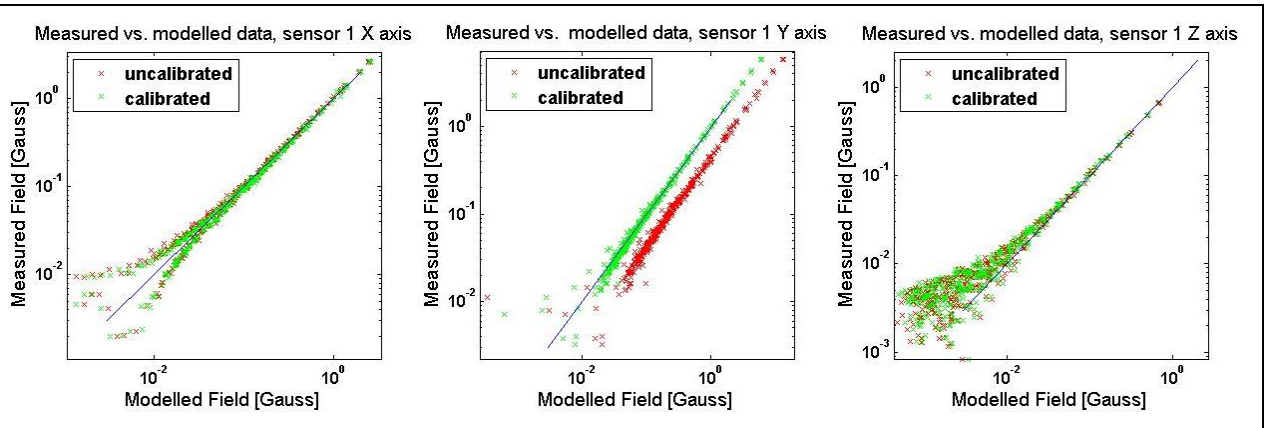

Figure 3: Measured vs. modelled magnetic fields before and after calibration, log-log scale

The above figure shows the results of the calibration for experimentally collected data. The x and z axis sensors were already well calibrated from the original manufacturer's calibration, however the y axis had a scaling factor that was corrected. The measured and expected values from the dipole model are in close agreement for measurements larger than approximately 50 milligauss. Calibration results using a different sensor were similar and showed roughly the same increase in model fit.

RESULTS AND DISCUSSION

Simulation Studies

A simulator was developed in MATLAB which implemented the sensor and experimental error models to generate simulated measurements from the dipole model. This simulator allows user control over the tracking workspace and for each of the variables in the error models given by Equations 4-6. Figure 4 shows the result of a simulated tracking experiment where the only source of error was the sensor resolution of 3 mg, which sets the smallest measurable difference in magnetic fields. The RMS position error passed the useful limit of 5 mm in the range of 20-25 cm distance between the sensor and the magnet. The field of a permanent magnet begins to approach that of a dipole in the far field, which as shown in Equation 1 is a propotional to the cube of the magnet to sensor distance. It is not surprising then that the small sensor resolution limit is quickly reached when sampling farther from the magnet.

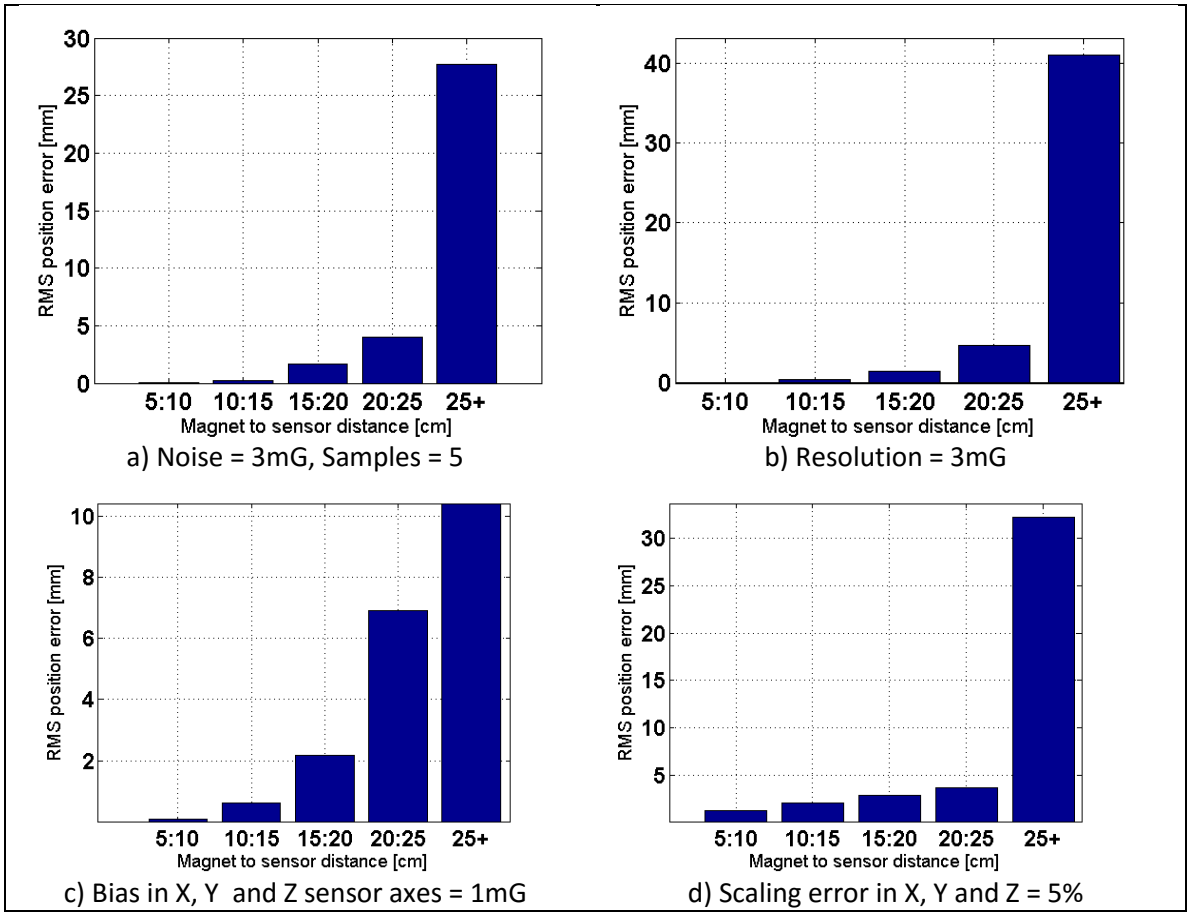

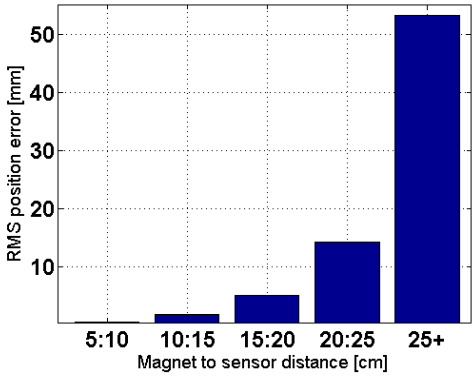

e) Magnet orientation error of 0.5 degrees around X, Y and Z axes, sensor resolution = 3mG

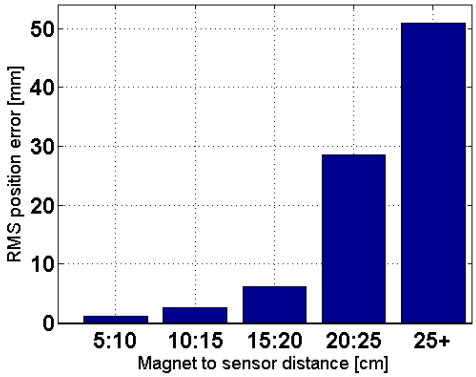

f) Magnet orientation error of 1 degree around X, Y and Z axes, sensor resolution = 3mG

Figure 4: Summary of results of simulations showing RMS position error between 5 to >25 cm sensor to magnet distance. All error parameters are zero except as stated in figure descriptions.

Position Tracking Experiments

The simulation results suggest that with a single magnet and sensor, a tracking accuracy in a practically large enough field would not be achieved and it is advisable to use more magnets and sensors. Ideally, one would devise a ring of many magnets around the workspace and use multiple sensors affixed to a rigid body, which is a clearly impractical proposition. Instead, we conducted testing with two sensors placed 4 cm apart.

The simulated tracking results found that small systematic errors in the presumed position and orientation of the magnet and sensors resulted in large increases in position error. We found poor tracking results initially compared to what was simulated, and was realized that accounting for these errors was necessary to be able to measure the tracking performance to the accuracy desired. Using calibration method described earlier, the position and orientation errors of the magnet and sensors were found using a non-linear optimization to minimize the error between the measured and modelled data. The results of this calibration are shown below.

Table 1: Calibration Parameters used in the position tracking experiments

	Euler Angles ϕ, θ, ψ [deg]	Position Error in x, y, z [mm]	Sensor Scaling Factor in x, y, z
Magnet Errors	0.003, 0.0, 0.003	-1.5, -0.17, 0.008	N/A
Sensor One Errors	-0.47, -0.08, 0.56	-0.08, 0.33, -0.07	1.00, 1.00, 1.02
Sensor Two Errors	-0.32, -0.30, 0.61	-0.03, 0.34, -0.07	1.00, 1.00, 1.02

While the calibration errors appear small, insights gained from simulations suggest they are sufficiently large to measurably impact the tracking performance. The position tracking performance, shown in Figure 5, suggests that at best the tracking error was over 5 mm at distances between 10 and 15 cm from the magnet, a lower accuracy than the simulated results. Both sensors show similar tracking accuracy, with a rapid drop in accuracy after 10 to 15 cm.

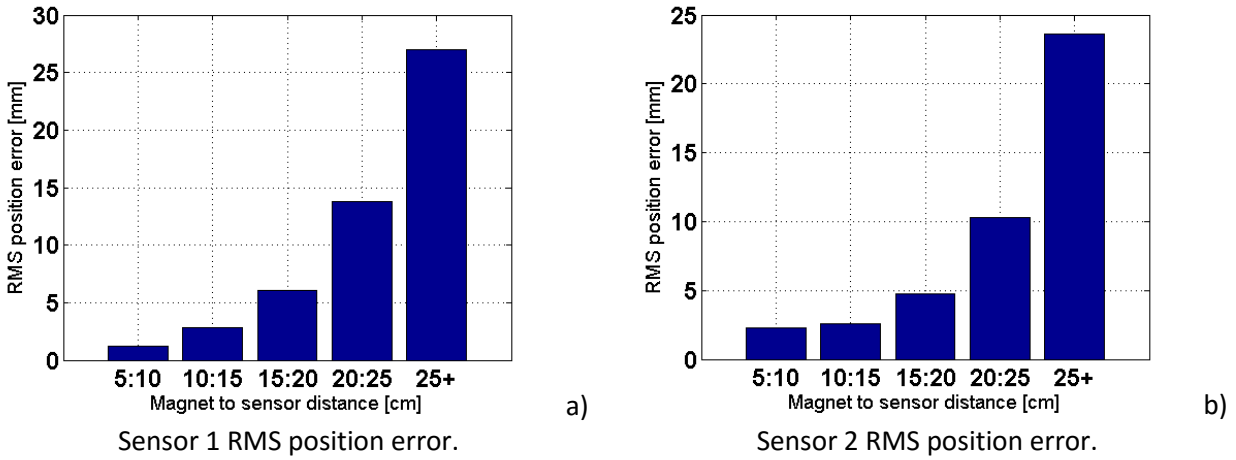

Sensor 1 RMS position error. Sensor 2 RMS position error.

Figure 5: RMS position error from tracking with sensor 1 (a) and sensor 2 (b).

As most reported permanent magnet tracking solutions use many sensors, tracking was extended to use both sensors simultaneously. The tracking performance of this method is shown in Figure 6 in terms of RMS error of the tracking with both sensors. The tracking range is not noticably improved when the magnet is far from both sensors. Along the X-axis however the magnet is between 2 and 4 cm closer to one sensor or the other at any given point, and in this region the tracking is improved. So long as the magnet is within 10 cm of at least one sensor, errors under 5 mm can be expected. The distance from the magnet to sensors here is calculated as the average of the distance to both sensors. There is not a large improvement overall, rather for any given distance the error seems to be similar to that achieved by whichever sensor was more accurate in that distance range.

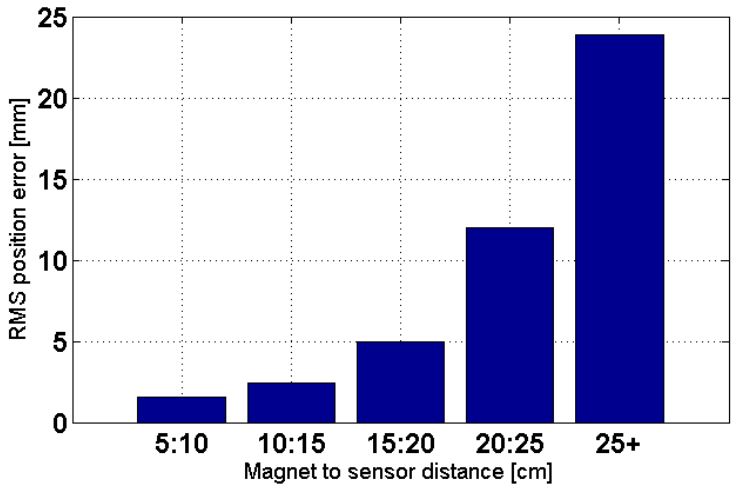

Figure 6: RMS position error for tracking with both sensors

CONCLUSIONS

The results shown here did not meet the desired tracking accuracy, yet many avenues of exploration remain to improve tracking results. The approach taken here attempted to use the same, or similar methods seen in previously published work. Given the lack of success it may be beneficial to approach novel methods to this problem. In investigating other avenues of research though it is important to bear in mind the overall goals of the system proposed here. The desire for low-cost and complexity is extremely important for the potential adoption of this system. In medical settings where clinicians and assistants do not have infinite time per patient, keeping calibration and setup time small is important. Additionally, small and unobtrustive trackers that are simple to mount to existing ultrasound probes will make their use less frustrating and more likely to be adopted. If the system is as large and expensive as existing tracking technologies it would be unlikely to be used. It is due to the desire to keep the system as small and simple (computationally, and in physical setup) as possible that the number of sensors used is kept to the lowest possible. Systems with high numbers of sensors and low sensor to magnet distances have been demonstrated , but go against the spitit of this work which was to develop a system which is as small and simple as possible. Computation time is also important, as most tracked ultrasound procedures (such as needle placement) require real time tracking.

From the insights gained in simulated tracking experiments, and from the experiences gained in tracking with real world data, it is clear that simple magnetic tracking systems are not currently capable of providing the accuracy and workspace to be clinically useful. The useful workspace in experimental tracking was limited to 20 cm from the magnet. This study also carefully eliminated the background field of the earth by keeping sensors stationary. In more practical systems this represents a large error source that cannot be trivially removed without careful calibration and sensor setup. Again, adding more sensors to reduce the average sensor to magnet distance would likely improve performance but results in more expensive systems with bulky sensor arrays which are not desirable to use with portable ultrasound devices.

REFERENCES

[1] W. Weitschies, R. Kötitz, D. Cordini and L. Trahms, "High-resolution monitoring of the gastrointestinal transit of a magnetically marked capsule," *Journal of Pharmaceutical Sciences*, 86, 1218-1222 (1997)

[2] C. Hu, M. Li, S. Song, W. Yang, R. Zhang and M. Q. H. Meng, "A Cubic 3-Axis Magnetic Sensor Array for Wirelessly Tracking Magnet Position and Orientation," *IEEE Sensors Journal*, 10(5), 903-913 (2010)

[3] J. Moré, "The Levenberg-Marquardt Algorithm: Implementation and Theory," *Lecture Notes in Mathematics*, 630, 115-116 (1978)

[4] MATLAB, "Equation Solving Algorithms - MATLAB & Simulink," Mathworks Inc. http://www.mathworks.com, (2015)